Transcription Factor RAP2.2 and Its Interacting Partner SINAT2: Stable Elements in the Carotenogenesis of Arabidopsis Leaves[1][W]

Ralf Welsch*, Dirk Maass, Tanja Voegel, Dean DellaPenna, and Peter Beyer

Faculty of Biology, Center for Applied Biosciences, Universität Freiburg, 79104 Freiburg, Germany (R.W., D.M., T.V., P.B.); and Department of Biochemistry and Molecular Biology, Michigan State University, East Lansing, Michigan 48824 (D.D.)

The promoter of phytoene synthase, the first specific enzyme of carotenoid biosynthesis, shows two main regulatory regions: a G-box-containing region located near the TATA box, and a TATA box distal region containing the cis-acting element ATCTA, which mediates strong basal promoter activity. This second element was also present in the promoter of phytoene desaturase, the next step of the carotenoid pathway, suggesting a common regulatory mechanism. In this work, we demonstrate that AtRAP2.2, a member of the APETALA2 (AP2)/ethylene-responsive element-binding protein transcription factor family, binds to the ATCTA element. In Arabidopsis (*Arabidopsis thaliana*) leaves, *AtRAP2.2* transcript and protein levels were tightly controlled as indicated by unchanged transcript and protein levels in T-DNA insertion mutants in the *AtRAP2.2* promoter and 5′ untranslated region and the lack of change in AtRAP2.2 protein levels in lines strongly overexpressing the *AtRAP2.2* transcript. Homozygous loss-of-function mutants could not be obtained for the *AtRAP2.2* 5′ untranslated region T-DNA insertion line indicating a lethal phenotype. In *AtRAP2.2* overexpression lines, modest changes in phytoene synthase and phytoene desaturase transcripts were only observed in root-derived calli, which consequently showed a reduction in carotenoid content. The RING finger protein SEVEN IN ABSENTIA OF ARABIDOPSIS2 (SINAT2) was identified as an AtRAP2.2 interaction partner using a two-hybrid approach. The structure of SINAT2 and related proteins of Arabidopsis show homology to the SEVEN IN ABSENTIA protein of *Drosophila* that is involved in proteasome-mediated regulation in a variety of developmental processes. The action of SINAT2 may explain the recalcitrance of AtRAP2.2 protein levels to change by altering AtRAP2.2 transcription.

Carotenoids fulfill important functions in photosynthesis, including harvesting of light energy and protection from damage by excess light energy (for a recent review, see Szabó et al., 2005). Accordingly, illumination of etiolated seedlings leads to the induction of carotenoid synthesis, coordinated with the synthesis of chlorophylls. Molecular analysis of this process revealed that the first committed enzyme of the carotenoid biosynthesis pathway, phytoene synthase (PSY), is strongly light induced both at the mRNA and protein levels in seedlings of mustard (*Sinapis alba*) and Arabidopsis (*Arabidopsis thaliana*; von Lintig et al., 1997; Welsch et al., 2000). In contrast, the mRNA and protein levels of enzymes acting upstream and downstream of PSY in the pathway, such as geranylgeranyldiphosphate synthase and phytoene desaturase (PDS), respectively, remained relatively constant. A key role for PSY may not be restricted to deetiolation and green tissues. It has recently been shown that carotene desaturation and lycopene cyclization are not rate limiting in carotenoid synthesis in Golden Rice (Al-Babili et al., 2006) and that PSY activity plays the major role (Paine et al., 2005).

Because of its crucial regulatory role of PSY in the carotenoid pathway, the PSY promoter region was analyzed in more detail (Welsch et al., 2003). This revealed two main regions that are responsible for the regulation of transcriptional activities. A TATA box proximal region containing G-box-like elements is involved in light induction and discrimination between different light qualities. A TATA box distal region enables a high basal level of promoter activity. Using gel retardation assays, the pentameric sequence ATCTA, occurring in tandem in the TATA box distal region, was identified as the cis-acting element for a transcription factor mediating strong *PSY* promoter activity. Interestingly, this novel motif is also found in promoter regions of other carotenogenic genes (i.e. *PDS* from tomato [*Lycopersicon esculentum*] and photosynthesis-related genes, such as the chlorophyll *a*/*b*-binding protein [*CAB*] of mustard and Arabidopsis and plastocyanin of pea [*Pisum sativum*]). The formation of protein-DNA complexes with the same migration pattern was observed with all these promoter regions containing the ATCTA motif. In addition, the complex formed with the *CAB*-mustard promoter element could compete with the

[1] This work was supported by the EC project ProVitA and by the HarvestPlus (www.harvestplus.org) research consortium.

* Corresponding author; e-mail welschra@web.de.

The author responsible for distribution of materials integral to the findings presented in this article in accordance with the policy described in the Instructions for Authors (www.plantphysiol.org) is: Ralf Welsch (welschra@web.de).

[W] The online version of this article contains Web-only data.
www.plantphysiol.org/cgi/doi/10.1104/pp.107.104828

PSY-Arabidopsis promoter element containing the ATCTA motif, indicating that the same transcription factor was involved.

These observations support the notion that the trans-acting factor involved might be able to regulate several genes involved in carotenogenesis, thereby also coordinating the expression of genes involved in photosynthesis. This, plus the proven importance of PSY in the carotenoid biosynthetic pathway, prompted us to identify cis-acting factors that govern the level of the basal *PSY* transcriptional activity using Arabidopsis as a model system.

RESULTS

South-Western Screening

Transcription factors that bind to cis-acting elements defined in the *PSY* promoter are unknown to date. To identify transcription factors binding to the previously identified upstream element (Welsch et al., 2003), we subjected a cDNA library of Arabidopsis to South-western screening. We used concatemers of the sequence 5′-CA**ATCTA**AAT**ATCTA**AAATATAAA-3′ as a probe, defined previously as a specific competitor of the protein-DNA complexes in gel retardation assays (Welsch et al., 2003). A λZAPII cDNA library of Arabidopsis (Kieber et al., 1993) comprising cDNAs of 1 to 2 kb in size was screened in parallel under two conditions. For binding of the probe to the bacteriophage plaques, screening was performed under native conditions and after chaotropic denaturation/renaturation of the recombinant proteins (Vinson et al., 1988). The screening process revealed reproducible signals. In vivo excision and sequencing resulted in the identification of a sequence identical to the transcription factor RAP2.2 from Arabidopsis (AtRAP2.2), an uncharacterized member of the family of APETALA2 (AP2)/ethylene-responsive element-binding protein (EREBP) transcription factors (AGI no. At3g14230; accession no. NM_180252).

Binding Assay with Recombinant AtRAP2.2

To confirm that AtRAP2.2 binds to the cis-acting element characterized in gel retardation experiments and used in South-western screening, gel retardation assays were performed with the recombinant protein. For this, *AtRAP2.2* cDNA was subcloned into the expression vector pQE30, thereby providing the recombinant protein with an N-terminal 6×-His tag. Purification of the recombinant protein via metal affinity under native conditions was not possible and gel retardation assays using the bacterial lysate failed due to accumulation of the recombinant protein in inclusion bodies (data not shown). Therefore, a chaotropic denaturation/renaturation procedure was applied following the conditions used during the screening. The use of renatured bacterial lysate containing recombinant AtRAP2.2 and the −856 to −825 region of the *PSY* promoter as a radiolabeled probe revealed the formation of a protein-DNA complex that could be competed specifically (Fig. 1). Compared to the control complex formed with nuclear extracts from illuminated mustard seedlings (as in Welsch et al., 2003), the complex formed with recombinant AtRAP2.2 migrated slightly differently. This is probably due to the N-terminal 6×-His tag influencing electrophoretic mobility of the complex.

Effects of Changed AtRAP2.2 Transcript Amounts in Arabidopsis

Transgenic AtRAP2.2-overexpressing lines were produced in Arabidopsis (ecotype Wassilewskija) to study the regulation of carotenoid biosynthesis and possible effects on expression of other photosynthesis-related genes. *AtRAP2.2* cDNA was expressed under the control of a strong promoter containing four tandem cauliflower mosaic virus (CaMV) enhancer elements (4CaMV-35S). The weaker *nos* promoter (*nosP*) was also used to create low expressing lines. From several transgenic lines, one homozygous line of each transformation was selected, grown under short-day conditions, and rosette leaves were harvested for further analyses. Real-time reverse transcription (RT)-PCR indicated that, relative to wild-type leaves, the

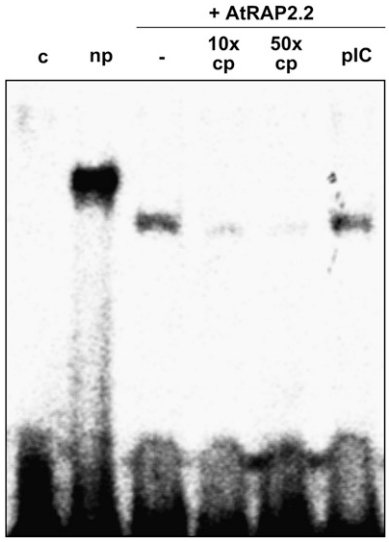

Figure 1. Gel retardation assay with recombinant AtRAP2.2. Gel retardation assays with lysates of *E. coli* cells expressing 6×-His-AtRAP2.2 were used to confirm the binding of AtRAP2.2 to the identified cis-acting element (+AtRAP2.2). Specificity was demonstrated with unlabeled competitor DNA added in 10- and 50-fold molar excess of the radiolabeled probe. The addition of nonspecific competitor DNA poly[d(I-C)] (pIC) had no effect on complex formation. Lysate from *E. coli* cells transformed with empty vector was used as negative control (C). Complexes formed with nuclear proteins isolated from light-grown mustard seedlings (np) show slightly different migration behavior compared to the complexes formed with recombinant 6×-His-AtRAP2.2, which is probably due to the effect of the charged His residues under native gel conditions.

AtRAP2.2 expression level was increased about 2-fold in the weak overexpressing line (*nosP*::*AtRAP2.2*; *nosr-2*) and almost 12-fold in the strong overexpressing line (*4CaMV-35S*::*AtRAP2.2*; *cmr-5*; Fig. 2B, left).

To investigate the effects caused by loss of AtRAP2.2 function, we took advantage of two T-DNA insertion lines, disrupted within the *AtRAP2.2* gene (Fig. 2A). One line, *rap*Δ*pro*, carried a T-DNA in the TATA box proximal region, leaving an intact minimal promoter of only 130 bp. However, *AtRAP2.2* transcript levels in homozygous *rap*Δ*pro* rosette leaves were relatively unchanged (Fig. 2B), indicating that the remaining intact promoter region provided sufficient activity to allow the accumulation of AtRAP2.2 transcript comparable to wild-type levels. The second T-DNA insertion line, *rap*Δ*utr*, contained the T-DNA within the 5′ untranslated region (UTR) of the *AtRAP2.2* transcript (leaving 60 bp of the 5′ UTR). However, unlike *rap*Δ*pro*, homozygous progeny for *rap*Δ*utr* could not be identified, even after repeated analyses of several generations of T3 progeny, indicating that loss of AtRAP2.2 function is lethal for embryo/seed development. Analysis of *AtRAP2.2* transcript levels in rosette leaves of heterozygous *rap*Δ*utr* progeny revealed almost no difference compared to wild type. Because the recessive loss-of-function *rap*Δ*pro* allele is lethal, it was not included in further analysis.

The two *AtRAP2.2*-overexpressing lines and two T-DNA insertion lines showed no apparent phenotypic differences compared to wild-type plants. Analysis of the carotenoid and chlorophyll content by HPLC revealed almost unchanged pigment content and patterns (Fig. 2F, left) and quantification of *PSY* and *PDS* transcript levels by real-time RT-PCR also revealed relatively unchanged mRNA levels compared to the wild type (Fig. 2, D and E, left). However, the two overexpressing lines did show strongly increased AtRAP2.2 transcript levels. To determine whether this increase in transcript level translated to an increase in AtRAP2.2 protein, antibodies directed against AtRAP2.2 were generated to conduct western-blot analyses.

Properties of AtRAP2.2

For antibody production, a glutathione *S*-transferase (GST) fusion protein of the N-terminal 166 amino acids of AtRAP2.2 was used as antigen because sufficient amounts of full-length AtRAP2.2 protein could not be produced in different bacterial (6×-His tag; GST) and yeast (*Saccharomyces cerevisiae*) expression systems. Western-blot analyses using total protein extracts from Arabidopsis wild-type rosette leaves yielded a signal with an apparent molecular mass of about 60 kD, whereas the calculated molecular mass of AtRAP2.2 is only 42.1 kD (Fig. 3). The same unexpected migration behavior was observed when AtRAP2.2 cDNA was translated in vitro in the presence of [^{35}S]-Met, both in reticulocyte lysate (RL) and wheat (*Triticum aestivum*) germ (WG) lysate (lane 1 RL and 1 WG, respectively). Strongly denaturing conditions applied by using urea-containing loading buffer did not result in a change of electrophoretic mobility (lane 1 WGU). To confirm that the antibodies generated specifically recognize AtRAP2.2, western-blot analyses were performed with the in vitro-translated product. This revealed a signal identical to those detected in the autoradiograms of the corresponding in vitro translations. Taken together, this proves that the western-blot signals obtained with protein extracts from leaves correspond to the authentic AtRAP2.2. Furthermore, we partially purified AtRAP2.2 from wild-type Arabidopsis nuclear protein extracts by DNA affinity chromatography. For this, concatemers of the sequence used in the South-western screening described above were coupled to Sepharose. Chromatography and subsequent SDS-PAGE revealed one dominant band migrating at a molecular mass of 60 kD.

Because AtRAP2.2 shows higher apparent molecular mass than expected in SDS-PAGE, we investigated the structural nature of this migration behavior by examining the apparent molecular masses of different truncated forms of AtRAP2.2 produced as in vitro-translated [^{35}S]-labeled proteins. Higher than expected masses were still observed when the AP2 domain was deleted (Fig. 3, lane 2 WG, RAPΔ109–192; calculated molecular mass 32.5 kD, apparent molecular mass 45 kD) and when only the N-terminal 250 amino acids were translated (lane 3 WG, RAP1–250; calculated molecular mass 28.7 kD; apparent molecular mass 37 kD). However, the expected molecular mass was obtained for the N-terminal 166-amino acid translation product (lane 4 WG, RAP1–166, calculated and apparent molecular masses 18.8 kD). Therefore, the region between amino acids 192 and 250 is the source of the electrophoretic discrepancies observed. The primary and secondary structure of this region does not suggest a basis for the altered electrophoretic mobility of AtRAP2.2 and no distinguishing domains or motifs were identifiable within this domain.

Unchanged Protein Amounts in Leaves of AtRAP2.2-Overexpressing Arabidopsis Lines

No apparent differences in AtRAP2.2 protein levels were detected (at the authentic electrophoretic mobility of 60 kD) in leaves of *AtRAP2.2*-overexpressing lines and the T-DNA insertion line *rap*Δ*pro* (Fig. 2). Whereas this was expected, with the latter considering its relatively unchanged transcript levels, it was surprising that the 12-fold increase in transcript levels in the *AtRAP2.2*-overexpressing line *cmr-5* would not lead to an increase in protein levels. This finding provides an interpretation of Affymetrix ATH1 GeneChip expression analyses run using total RNA isolated from leaves from the two overexpressing lines and the Wassilewskija wild type (see Table I). When using a 2.5-fold difference in all transgenic-to-wild type chip-to-chip comparisons as a filter, only six and four genes showed significant changes in the *nosr-2*- and *cmr-5*-overexpressing lines, respectively. Out of these genes,

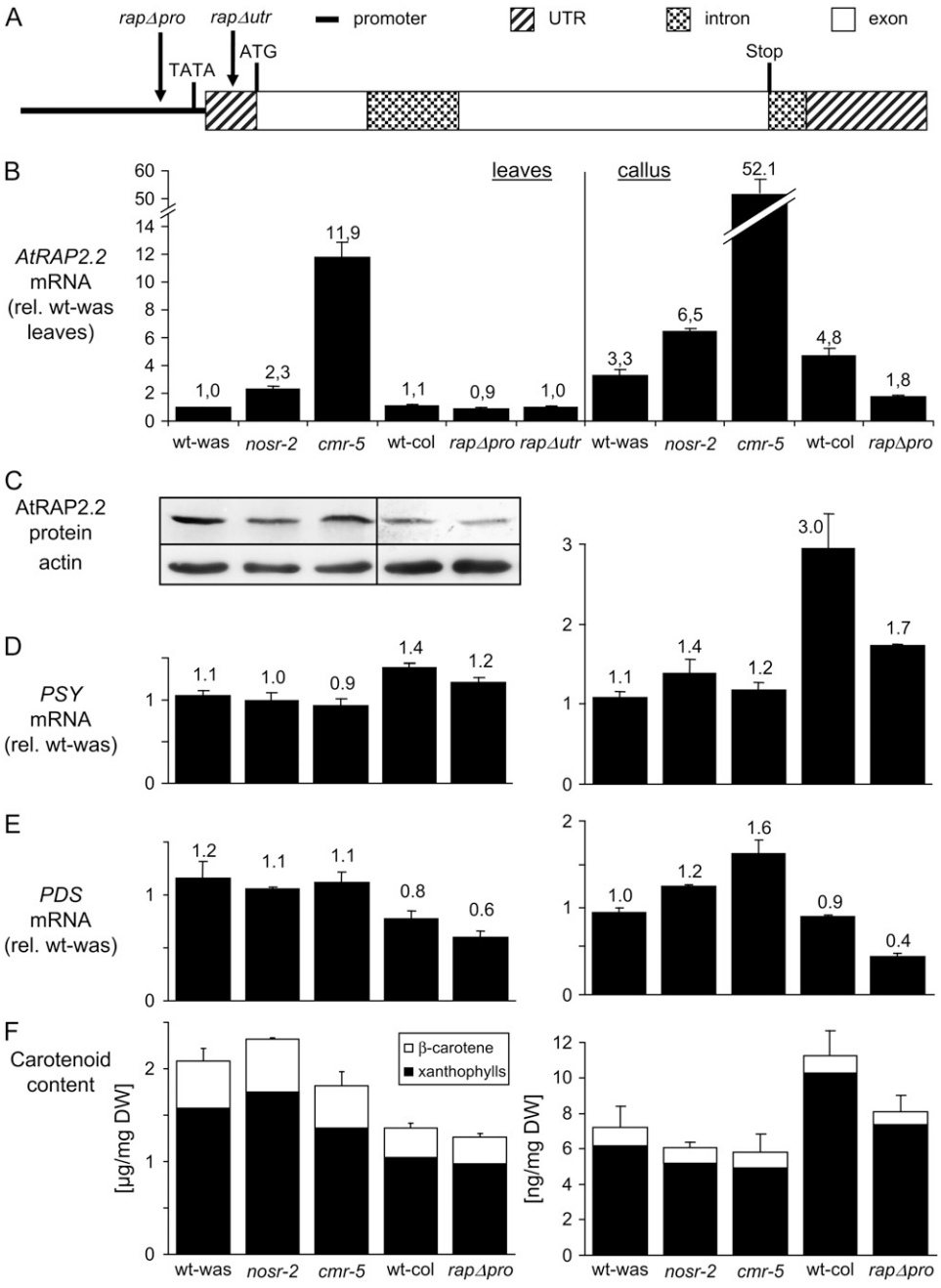

Figure 2. Effect of modified *AtRAP2.2* transcription levels in leaves and calli generated from roots. A, Schematic map of the *AtRAP2.2* T-DNA insertion mutations with the positions of T-DNA insertions in *rapΔpro* (SAIL 184 G12) and *rapΔutr* (SAIL 18 G09) indicated. Expression levels of *AtRAP2.2* (B), *PSY* (D), and *PDS* (E) in Arabidopsis rosette leaves (left) and root-derived callus (right) as determined by real-time RT-PCR. Lines overexpressing *AtRAP2.2* under control of the *nos* promoter (*nosr-2*) or the *CaMV-35S* promoter (*cmr-5*), respectively, are in the Wassilewskija background; the wild type is shown as control (wt-was). T-DNA insertion lines carrying insertions in the *AtRAP2.2* gene (*rapΔpro* homozygotes and *rapΔutr* heterozygotes) are in the Columbia-0 background; the wild type is shown as a control (wt-col). Transcript levels were first normalized relative to 18S rRNA expression levels and are expressed relative to the expression level of the Wassilewskija wild-type leaves from one replicate. Normalized *PSY* and *PDS* expression levels are expressed relative to the expression levels of the corresponding tissue (leaves and callus, respectively) detected in Wassilewskija wild type from one replicate. Data represent the average and SE (error bars) of two biological replicates. C, Protein levels of AtRAP2.2. Western-blot analysis of AtRAP2.2 protein levels using 40 μg of leaf protein extracts and anti-AtRAP2.2 antibodies. The protein levels of actin are shown as a loading control. F, Carotenoid content in leaves and root calli as determined by quantitative HPLC. For further explanation, see text.

only two plastid-encoded genes occurred in both datasets, the PSI assembly protein, *ycf*4, and the ATPase I subunit, *atp*F. Additional differently expressed genes in the weak overexpressing line, *nosr-2*, belong to processes involved in RNA and protein regulation. Analysis of the datasets using less stringent parameters increased the number of differently expressed genes more than 10-fold in both datasets (see Supplemental Table S1, A and B), but the list of genes affected in both *nosr-2* and *cmr-5* only increased by two genes (see Supplemental Table S1C). These expression analyses are consistent with the observation that in photosynthetically active tissues AtRAP2.2 protein levels cannot be altered by increasing AtRAP2.2 transcript levels and therefore no pronounced changes in the transcriptome result from AtRAP2.2 overexpression.

Effects of AtRAP2.2-Overexpressing Arabidopsis Lines on Root-Derived Calli

Numerous transgenic experiments in various plant systems have demonstrated that photosynthetically active tissues/cells are more recalcitrant to attempts to engineer carotenoid flux and content than nongreen tissues/cells (for a recent review, see Howitt and Pogson, 2006). Therefore, we analyzed callus tissue

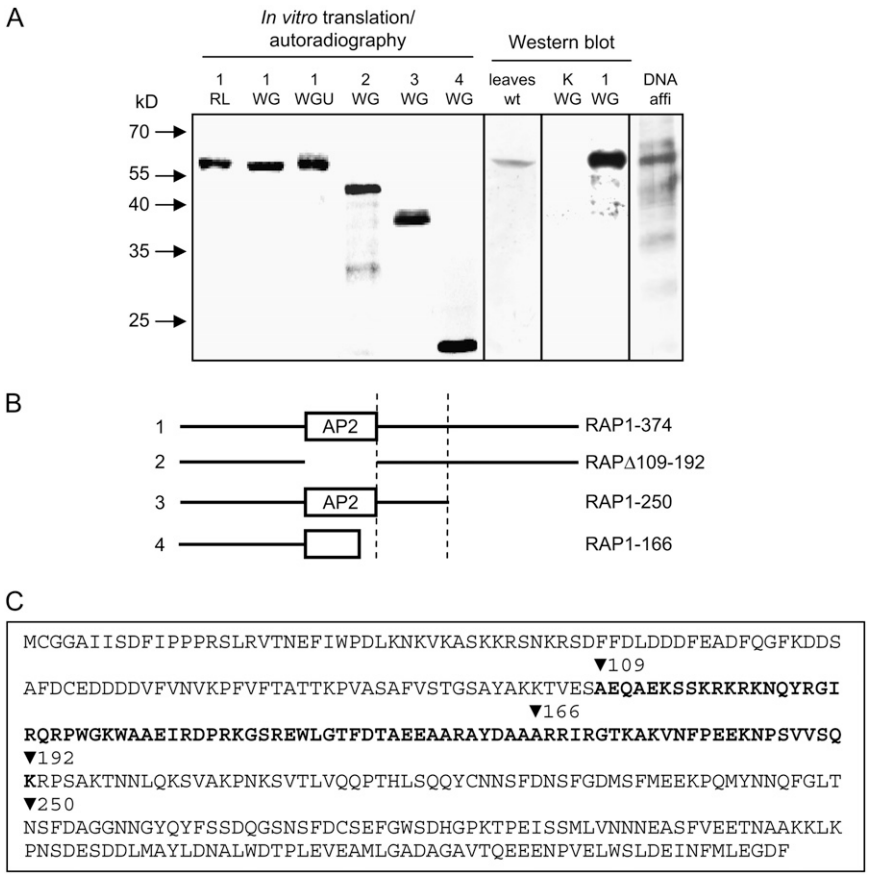

Figure 3. Migration behavior of AtRAP2.2 in SDS-PAGE. A, Autoradiography of in vitro translation products of different AtRAP2.2 truncations (left). Western-blot analysis using anti-AtRAP2.2 antibodies and a silver stain of proteins obtained by DNA affinity chromatography is shown on the right. B, Schematic representation of the truncations used in A; the region responsible for the unusual migration behavior observed is marked between dashed lines. C, Amino acid sequence of AtRAP2.2. The AP2 domain is shown in bold; arrowheads indicate the amino acid positions used for the truncations in B. The calculated mass of AtRAP2.2 is 42.1 kD; however, an apparent molecular mass of about 60 kD is observed in western-blot analyses using 40 μg of leaf protein extracts and anti-AtRAP2.2 antisera (leaves wt). The [^{35}S]Met translation products of the *AtRAP2.2* cDNA showed the same electrophoretic mobility in RL (1 RL) and WG lysate (1 WG). The presence of urea in the loading buffer did not influence this behavior (1 WGU). Deletions lacking the AP2 domain (2 WG, RAPΔ109–192; calculated molecular mass, 32.5 kD; apparent, 45 kD) and truncation of the C-terminal 124 amino acids (3 WG, RAP1–250; calculated molecular mass, 28.7 kD; apparent, 37 kD) also showed anomalous electrophoretic mobility. The expected molecular mass was observed for the N-terminal 166 amino acids (4 WG, RAP1–166, calculated and apparent molecular mass, 18.8 kD). Western-blot analysis conducted with the in vitro translation product showed a signal identical to that observed in the autoradiography of the same sample (1 WG), whereas an in vitro translation performed with the empty vector pGEM4 showed no signal (K WG). Using concatemers of the sequence used for the screening of AtRAP2.2 and nuclear proteins of Arabidopsis leaves, DNA affinity chromatography was performed. Silver staining revealed selective enrichment of AtRAP2.2 in the eluate (DNAaffi).

generated from roots of the AtRAP2.2-overexpressing lines (Fig. 2, right). Here, the weak overexpressing line, *nosr-2*, and the strong overexpressing line, *cmr-5*, showed a 2- and 17-fold increase in *AtRAP2.2* transcript levels relative to wild-type levels. Western-blot analysis to investigate AtRAP2.2 protein amounts in callus failed because protein amounts were below the detection limit in all cases. However, if the increase in *AtRAP2.2* transcript amounts correlated with an increase in protein amounts in this tissue, one would expect a detectable signal, at least with the high expressing line. We assumed that in root-derived calli—just as in leaves—AtRAP2.2 protein amounts were being kept at a low steady-state level and that there was no linear correlation between transcript and protein amounts. Consistent with this assumption, *PSY* expression levels and the carotenoid content of *nosr-2* and *cmr-5* were similar to wild type (Fig. 2, D and F, right). Only *PDS* expression was slightly increased relative to the wild type (24% and 62% increase in *nosr-2* and *cmr-5*, respectively). This might represent effects caused by a small AtRAP2.2 increase.

In contrast to the overexpressing lines, root-derived calli generated from the T-DNA insertion line *rap*Δ*pro* carrying an insertion in the promoter region showed a significant decrease in *AtRAP2.2* transcript levels to

Table I. *Affymetrix ATH1 GeneChip analysis comparing expression levels in wild-type Arabidopsis leaves with those of two different AtRAP2.2-overexpressing lines*

Genes affected in leaves of the weak *AtRAP2.2*-overexpressing line *nosr-2* and the strong *AtRAP2.2*-overexpressing line *cmr-5*, respectively, are shown as fold induction/repression relative to wild-type leaves, each as the mean of two biological replicates. For analysis, data were filtered for flags present in three of four samples, followed by filtration for 2.5-fold difference between transgenic and wild-type lines. For data analysis with less stringent parameters, see Supplemental Table S1.

Gene Description	Fold-Change	Probe Set No.	AGI No.
Leaves of weak *AtRAP2.2*-overexpressing line *nosr-2* versus wild-type leaves			
Nucleoredoxin/PDI-related protein, putative receptor kinase	−2.6	253519_at	At4g31240
Transducin/WD40 repeat family protein, putative splicing factor	−2.5	263261_at	At1g10580
Cullin 3B, ubiquitin-protein ligase	−2.5	260416_at	At1g69670
Zinc (RING) finger family protein	−2.5	259800_at	At1g72175
PSI assembly protein, ycf4	3.2	245018_at	AtCg00520
ATPase I subunit, atpF	3.1	245025_at	AtCg00130
Leaves of strong *AtRAP2.2*-overexpressing line *cmr-5* versus wild-type leaves			
Exocyst subunit EXO70 family protein	2.4	247693_at	At5g59730
PSI assembly protein, ycf4	3.6	245018_at	AtCg00520
ATPase I subunit, atpF	3.1	245025_at	AtCg00130
Ribosomal protein L14, rpl14	2.5	244982_at	AtCg00780

about 35% of wild type (Fig. 2B, right). This difference relative to leaves (where transcript levels remained unchanged) may lie in the fact that *AtRAP2.2* mRNA levels in wild-type calli are 5-fold higher than in leaves. Therefore, the remaining promoter activity in *rap*Δ*pro* is sufficient to reach wild-type levels in leaves of *rap*Δ*pro*, but obviously too weak to provide the higher levels found in wild-type calli. Conclusions about AtRAP2.2 protein levels from western-blot analysis were not possible because they were below the detection limit.

Interestingly, the decrease in *AtRAP2.2* transcript levels in *rap*Δ*pro* was accompanied by significant reduction of both *PSY* and *PDS* transcripts to 50% of the wild-type level and was correlated with a 30% decrease in carotenoid content relative to wild-type calli (Fig. 2, D–F, right).

Interaction Partners of AtRAP2.2

The results presented so far led to the conclusion that AtRAP2.2—at least in leaves—is regulated mainly at the posttranslational level: Protein levels were unresponsive to changes in mRNA abundance. This might indicate that AtRAP2.2 protein is subjected to specific protein degradation, a process that involves protein-protein interaction.

To obtain information on possible AtRAP2.2 interaction partners, protein overlay assays using nuclear extracts from light-grown mustard seedlings were performed. For this, in vitro-translated [^{35}S]-labeled AtRAP2.2 and a radiolabeled C-terminal truncation, RAP1-250, were used. Both translation products recognized at least two proteins, both with a molecular mass of about 36 kD (Fig. 4).

In subsequent yeast two-hybrid screens, the entire *AtRAP2.2* cDNA was fused to the GAL4 activation domain of pGBT9 to yield pGBT9-RAP. Yeast Hf7c cells transformed with this construct alone were able to grow on synthetic dropout medium lacking Trp and His, which indicated autoactivation of the *HIS3* reporter gene. This is frequently observed with transcription factors and limits the use of the two-hybrid screen. Attempts to repress this autoactivation by the addition of the His biosynthesis suppressor 3-amino1,2,4-triazol were unsuccessful. Therefore, we set out to eliminate the responsible region by using truncated forms of AtRAP2.2 in an autoactivation growth test (Fig. 5). This revealed that AtRAP2.2 contains at least two regions that can independently act as autoactivation domains. One region is located in the C-terminal third between positions 252 and 374, because yeast transformed with pGBT9-RAP252–374 was able to grow on selective medium. The second region is located in the central third of the amino acid sequence between positions 166 and 250 because the N-terminal 250 amino acids of AtRAP2.2 (in pGBT-RAP1–250) show autoactivation, whereas the N-terminal 166 amino acids (in pGBT-RAP1–166) do not.

Because the RAP1–166-GAL4BD fusion protein was devoid of autoactivation activity, the construct pGBT9-RAP1–166 was used as the bait vector in the two-hybrid screen. An Arabidopsis library with cDNAs connected to the GAL4 activation domain in pGAD424 was used as the prey library: 3×10^6 yeast transformants were screened. After eliminating false-positive clones by confirming the interaction with RAP1–166 by reconstitution, by using the second reporter gene *lacZ*, and by testing possible autoactivation of the prey cDNAs alone, five positive clones were obtained. Restriction endonuclease digestion and DNA sequencing showed that they contained identical cDNAs corresponding to a 5′-proximal truncated cDNA of *SEVEN IN ABSENTIA IN ARABIDOPSIS2* (*SINAT2*; AGI no. At3g58040; accession no. AY087768.1). The result of these two-hybrid assays showed that AtRAP2.2

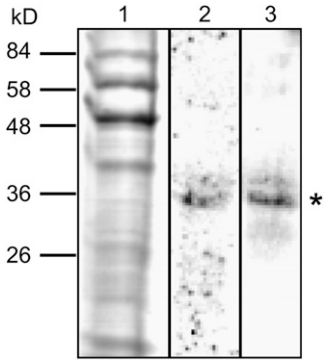

Figure 4. Interaction of AtRAP2.2 with nuclear proteins. Protein overlay assay using 40 μg of nuclear protein from light-grown mustard seedlings and [^{35}S]-labeled full-length AtRAP2.2 (lane 2) or the N-terminal 250 amino acids of AtRAP2.2 (lane 3). A Coomassie stain of the nuclear proteins used is shown in lane 1. AtRAP2.2 interacts with at least two nuclear-localized proteins with molecular masses of about 36 kD (indicated by an asterisk).

may interact with this particular gene product. The protein overlay assay described above demonstrated interaction between AtRAP2.2 and a protein of 35 kD, which corresponds to the molecular mass of SINAT2. Interestingly, SINAT2 contains a RING zinc finger motif involved in proteasomal-mediated degradation of proteins as part of many E3 ubiquitin ligases.

Identification of SINAT2 as Interaction Partner of AtRAP2.2

To verify the interaction of AtRAP2.2 with SINAT2, pull-down assays were carried out. The C terminus of SINAT2 was subcloned in the vector pGEX4T2 enabling the expression of an N-terminal GST-fusion protein (GST-SINAT2-C). After purification, pull-down assays were performed with [^{35}S]-labeled AtRAP2.2. As shown in Figure 6, GST-SINAT2-C interacted with AtRAP2.2, whereas GST alone did not. To repeat pull-down assays with the entire SINAT2 amino acid sequence, the full-length cDNA of *SINAT2* was cloned by RT-PCR using total RNA isolated from Arabidopsis leaves, subcloned into pGEX4T2, and expressed as N-terminal GST fusion protein as above (GST-SINAT2). The pull-down assay performed with GST-SINAT2 and [^{35}S]AtRAP2.2 confirmed the results obtained with the N-terminally truncated SINAT2, as shown in Figure 6.

This interaction of AtRAP2.2 and SINAT2 may explain the observed discrepancies between increased transcript amounts and unchanged protein amounts in leaves of *AtRAP2.2*-overexpressing lines described above. SINAT2 might target AtRAP2.2 for proteasomal degradation, ensuring constant steady-state AtRAP2.2 protein amounts, independent of transcript levels. Therefore, variations of SINAT2 transcript amounts might lead to more pronounced phenotypic effects than variations of AtRAP2.2 transcript amounts.

Analysis of SINAT2 T-DNA Insertion Lines

To investigate the effects of decreased *SINAT2* transcript amounts, a T-DNA insertion line was characterized that carries T-DNA within the second exon of the *SINAT2* gene (*sinat2*Δ; Fig. 7). If a stable transcript were produced in this line, it would contain a premature translational stop after amino acid 134 that would result in the deletion of both RING finger domains, rendering protein-protein interaction impossible. Homozygous *sinat2*Δ progeny showed no apparent phenotypic differences compared to wild type. As shown in Figure 7, neither rosette leaves nor root-derived calli from the homozygous *SINAT2* insertion line showed differences in carotenoid content or composition. Accordingly, transcript levels of *PSY*, *PDS*, and also *AtRAP2.2* remained almost unchanged in *sinat2*Δ compared to wild type. AtRAP2.2 protein amount was examined by western-blot analysis in leaves and was found to be unchanged as well. This unexpected result

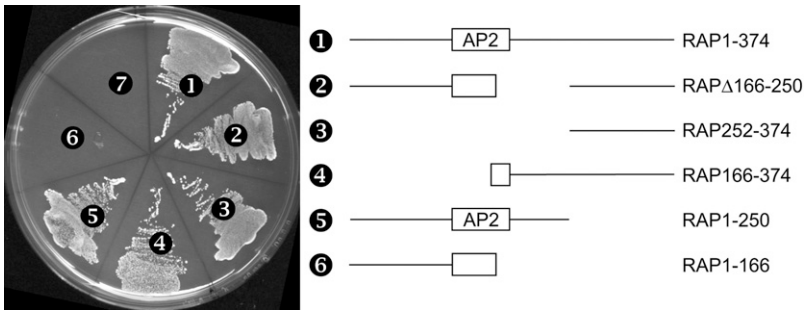

Figure 5. Autoactivation of reporter gene expression by different AtRAP2.2 truncations AtRAP2.2 (1) and different N- and C-terminal truncations (3–6) or deletions (2) of AtRAP2.2 were fused to the GAL4 binding domain of pGBT9, transformed into yeast strain Hf7c and tested for autoactivation by growing transformants on synthetic dropout medium lacking Trp and His. Number 7 represents empty vector (pGBT9) transformants as negative control. AtRAP2.2 contains at least two regions that can act as independent autoactivation domains. One region is localized between positions 252 and 374 (compare 2 and 3), whereas the second is located between position 166 and 250 (compare 4 and 5). Only pGBT9-RAP1/166 (6) showed no autoactivation activity and was for used for two-hybrid screening.

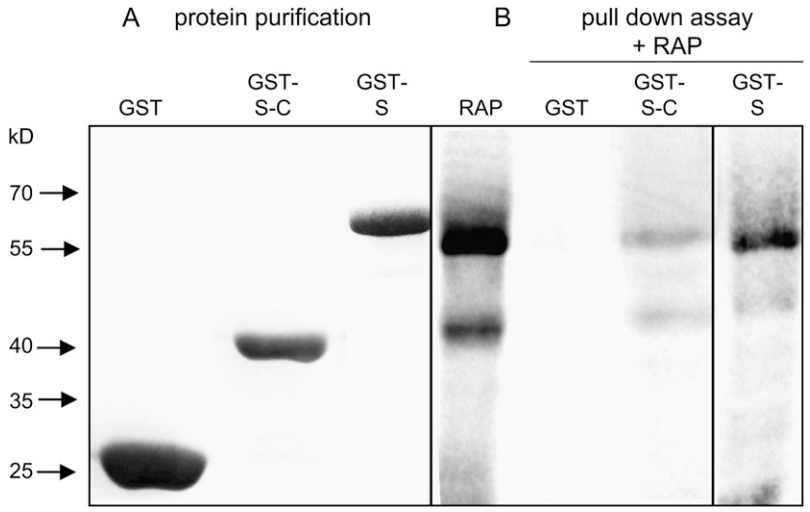

Figure 6. Pull-down assay. A, Protein purification: Coomassie stain of the purified C-terminal part of SINAT2 (amino acids 190–313), N-terminally fused to GST (lane GST-S-C). The full-length SINAT2 amino acid sequence, N-terminally fused to GST, is shown in lane GST-S and purified GST in lane GST. B, Pull-down assay with purified GST fusion proteins from A and [^{35}S]-labeled AtRAP2.2. The untreated translation product is shown in the first lane (RAP). Interaction between AtRAP2.2 and GST-S-C, as well as GST-S, is indicated by the appearance of radiolabeled AtRAP2.2 bands. A pull-down assay with [^{35}S]-AtRAP2.2 and GST alone is shown as negative control (GST).

may be due to the existence of four SINAT2 homologous proteins in Arabidopsis that may functionally substitute in this regard for the loss of function of SINAT2.

DISCUSSION

The cis-acting element ATCTA on the *PSY* promoter of Arabidopsis is responsible for high-level basal expression of the gene. Regulation of *PSY* promoter activity via this upstream element is independent of the G-box-like elements involved in light response (Welsch et al., 2003). Using the promoter region containing the ATCTA motif as a probe in South-western screening procedures, we isolated the transcription factor AtRAP2.2, a member of the large family of AP2/EREBP transcription factors (Riechmann and Meyerowitz, 1998) and verified its binding specificity by gel retardation assays. The ATCTA motif occurs in both the *PSY* and *PDS* promoters and is recognized by the same transcription factor, probably AtRAP2.2 (Welsch et al., 2003).

AtRAP2.2 Is an Essential Gene Whose mRNA Is Recalcitrant to Down-Regulation

Plant lines carrying a T-DNA insertion in the *AtRAP2.2* promoter region and in the 5′-UTR region were used to investigate the phenotypic effects of altering AtRAP2.2 expression. Surprisingly, down-regulation of *AtRAP2.2* mRNA could not be achieved in leaves. *rap*Δ*pro*, which carries a T-DNA insertion approximately 70 bp upstream of the putative TATA box, apparently maintains sufficient promoter activity to drive *AtRAP2.2* expression to wild-type levels. Homozygous *rap*Δ*pro* progeny are viable and with *AtRAP2.2* expression and visible phenotype indistinguishable from wild type. *rap*Δ*utr*, a second mutant allele that contains a T-DNA insertion in the 5′ UTR, produced heterozygous progeny with *AtRAP2.2* mRNA levels indistinguishable from wild type, could be recovered, but homozygous progeny were not viable. These data suggest *AtRAP2.2* is an essential gene and that negative impact on *AtRAP2.2* mRNA levels due to moderate down-regulation of transcription are avoided by feedback regulation of mRNA levels. The situation differs somewhat in nongreen tissues, such as root-derived calli where wild-type *AtRAP2.2* mRNA levels are 5 times higher than in leaves. In this tissue, the minimal promoter activity of the homozygous *rap*Δ*pro* mutant is not sufficient to attain the elevated level in wild type. This yielded the expected effects, namely, down-regulation of *PSY* and *PDS* expression (both of which carry the *AtRAP2.2*-binding motif in their promoters) and consequently decreased carotenoid levels.

AtRAP2.2 Interacts with SINAT2, a RING Finger Protein

In contrast to attempts to down-regulate AtRAP2.2 expression, AtRAP2.2 mRNA levels could be readily increased in overexpression experiments. However, despite greater than 10-fold increases in AtRAP2.2 mRNA levels in transgenics, AtRAP2.2 protein levels were unchanged. This might be due to an mRNA-based regulatory mechanism (e.g. miRNA; Aukerman and Sakai, 2003; Chen, 2004) because a computational approach taken by Wang and coworkers (2004) identified AtRAP2.2 as a target for a yet-uncharacterized miRNA (Wang et al., 2004). However, using the truncated RAP1–166 as bait, we identified the RING finger protein SINAT2 as an interaction partner of AtRAP2.2 and these data point to proteasome-mediated protein degradation as the underlying regulatory principle controlling AtRAP2.2 protein levels.

SINAT2 contains two zinc finger domains of different types (see Supplemental Fig. S1). One shows a RING-type profile and is located between amino acids 60 to 96; the second has a *SEVEN IN ABSENTIA HOMOLOG* (*SIAH*)-type profile and is located between amino acids 113 and 173. The SIAH-type domain

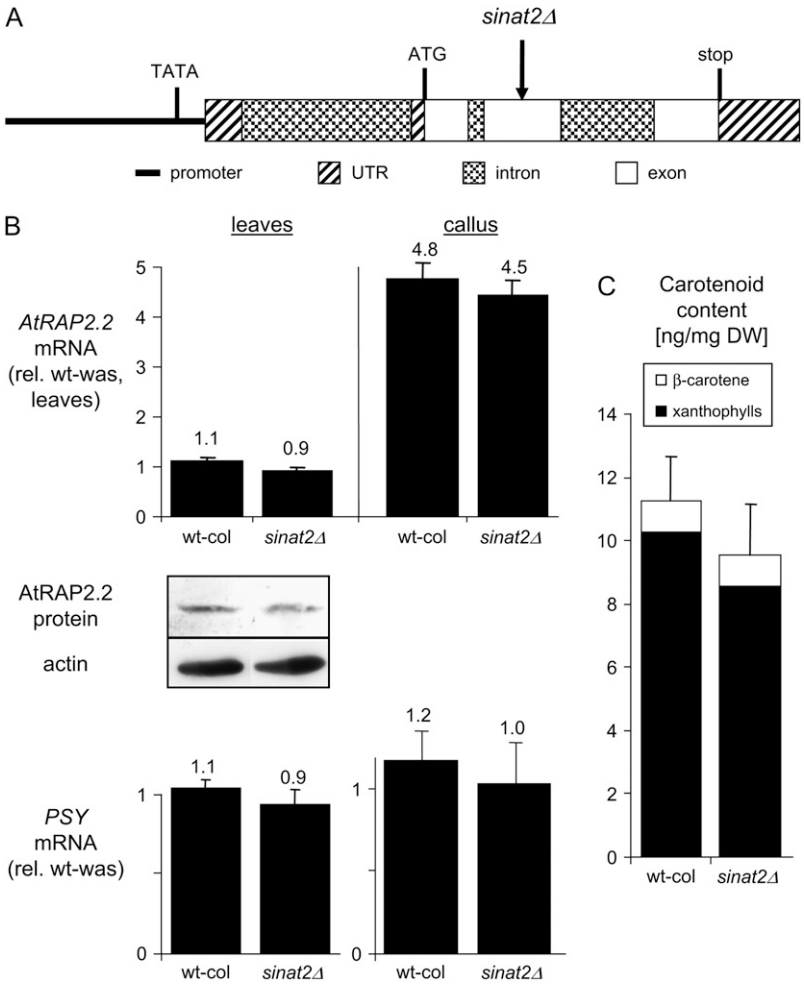

Figure 7. Analysis of the *SINAT2* T-DNA insertion line. A, Schematic map of the T-DNA insertion mutation in *SINAT2*. Arrow indicates the position of T-DNA insertion in *sinat2*Δ (SAIL 122 A04). B, Expression levels of *AtRAP2.2* (top) and *PSY* (bottom) in Arabidopsis rosette leaves and root-derived calli from wild-type plants (wt-col) and *sinat2*Δ as determined by real-time RT-PCR. Transcript levels were first normalized for 18S rRNA expression levels, then for the expression level of the corresponding wild-type levels. Data represent the average and SE (error bars) of two biological replicates. The western blot shows AtRAP2.2 protein levels using 40 μg of leaf protein extracts and anti-AtRAP2.2 antibodies. Protein levels of actin are shown as a loading control. C, Carotenoid content in root calli as determined by quantitative HPLC. For further explanation, see text.

defines a zinc finger type found in the *Drosophila* SEVEN IN ABSENTIA (SINA) protein and its mammalian orthologs. The *SINA* gene encodes a nuclear protein that is required for the correct development of R7 photoreceptor cells in the *Drosophila* eye (Carthew and Rubin, 1990). The architecture found in SINAT2—a RING-type zinc finger followed by a SIAH-type zinc finger—is found in a small group of five related proteins in Arabidopsis (SINAT1 to SINAT5; Xie et al., 2002).

The RING finger domain is related to the zinc finger domain family that represents one of the most abundant domains in the Arabidopsis proteome. In contrast to zinc finger domain-containing proteins, which are a functionally diverse group, the RING finger domain is generally considered to be involved in protein-protein interactions (Laity et al., 2001; Kosarev et al., 2002). Many RING finger proteins are involved in ubiquitinylation of substrate proteins to initiate their proteasome-mediated degradation. During this process, RING finger domain-containing proteins are constituents of E3 ligases that are ubiquitinylated by an E2 protein (ubiquitin-conjugating protein). Consecutively, transfer of the ubiquitin moiety to its substrate target proteins is mediated, a process that requires protein-protein interaction. RING domains are assumed to contribute to the scaffold by providing optimal positioning of E2 and the substrate for the transfer of ubiquitin (Zheng et al., 2002).

The regions involved in the interaction between AtRAP2.2 and SINAT2 were deduced from yeast two-hybrid screening and pull-down assays. Due to the autoactivating properties of the C-terminal half of AtRAP2.2, yeast two-hybrid screening was performed using the N-terminal 166 amino acids of the protein, which removed the C-terminal half of SINAT2. Interestingly, the C-terminal half of SINAT2 does not contain any of the two zinc finger domains, but the corresponding domain has been identified as the substrate-binding domain in SIAH and is thus involved in the recognition and binding of a variety of different protein substrates (Reed and Ely, 2002). Because most of the AP2 domain was included in the N-terminal part of AtRAP2.2 used for the screening and pull-down assays, it appears that SINAT2 and the other four SINAT2-homologous proteins present in Arabidopsis regulate additional AP2 domain-containing proteins via their C-terminal substrate-binding domain.

Several lines of evidence support the involvement of SINAT2 in protein degradation processes. SINAT5, a close homolog of SINAT2 in Arabidopsis, is involved in ubiquitin-mediated regulation of auxin-regulated developmental processes, as suggested by its in vitro ubiquitin protein ligase activity (Xie et al., 2002). Furthermore, both the *Drosophila* protein SINA and homologous mammalian proteins (SIAHs) are involved in the ubiquitin-mediated degradation of proteins with important functions in developmental processes (Li et al., 1997; Tang et al., 1997; Dong et al., 1999; Boulton et al., 2000). Therefore, it appears likely that SINAT2 is also an E3 ligase constituent acting on AtRAP2.2. Thus, the observation that AtRAP2.2 protein levels in leaves of *AtRAP2.2*-overexpressing lines are unchanged is best explained by a regulated protein degradation process involving SINAT2 that maintains a constant steady-state level of the protein despite alterations in mRNA levels. However, in leaves of *SINAT2* T-DNA knockout lines, the AtRAP2.2 protein amounts remain unchanged. Interestingly, the identity of the four other members of the Arabidopsis SINAT protein family to SINAT2 is very high (homology to SINAT1, 94.2%; SINAT3, 72.7%; SINAT5, 72.4%; SINAT4, 71.6%; see Supplemental Fig. S1). It is therefore conceivable that one or more of the members of this group are able to functionally compensate for SINAT2 in the SINAT2Δ line.

Given the resilience of AtRAP2.2 toward down-regulation at the mRNA level and toward up-regulation at the protein level, it is not surprising that the whole-genome microarray expression analyses conducted in parallel showed little variability. Expression of only six genes was changed in leaves of the weak *AtRAP2.2*-overexpressing line *nosr-2* when applying a minimal filter for expression changes of at least 2.5-fold in all pair-wise analyses of wild type. Furthermore, in comparison with the strong *AtRAP2.2*-overexpressing line *cmr-5*, no common nuclear-encoded genes were affected. Therefore, the slight changes in expression levels observed in leaves are most probably due to minor variations and do not represent an effect of the overexpression of *AtRAP2.2*.

AtRAP2.2: General Considerations

The AP2/EREBP family of transcription factors, to which AtRAP2.2 belongs, is classified according to the existence of one or two DNA-binding AP2 domains, initially characterized in AP2 (Weigel, 1995). Apart from the AP2 domains, homology is very low among almost all AP2/EREBP proteins. Recently, three groups presented data from other AP2 domain-containing transcription factors from tomato, tobacco, and barley (*Hordeum vulgare*), respectively, with 25% to 38% identity to AtRAP2.2 at the protein level.

For JERF1 from tomato, Zhang and coworkers demonstrated that this transcription factor binds to the GCC box and the DRE sequence in vitro, both of which are involved in stress responses (Zhang et al., 2004). Overexpression of JERF1 in tobacco led to increased expression of GCC box-containing genes in leaves under nonstressed growth conditions, consequently leading to enhanced salt stress tolerance. Lee and coworkers identified NtCEF1 from tobacco, which shows 68.5% identity to JERF1, and demonstrated its binding to the GCC box and the C/DRE element in vitro by gel retardation assays (Lee et al., 2005). However, only GCC box-containing genes were affected in vivo. Overexpression of *NtCEF1* in Arabidopsis led to enhanced resistance to a bacterial pathogen. Jung and coworkers reported that overexpression of HvRAF from barley in Arabidopsis also activated stress-responsive genes under nonstressed conditions and conferred enhanced pathogen resistance (Jung et al., 2007).

The question arises as to whether AtRAP2.2 represents the Arabidopsis equivalent of NtCEF1, JERF1, or HvRAF. Because of the generally low degree of homology among the members of the AP2/EREBP family, despite a common AP2 domain, functional equivalency based on homology is often difficult. Given this constraint, the 38% identity that AtRAP2.2 shares with JERF1 and NtCEF1 is relatively high. However, the main argument against AtRAP2.2 being functionally equivalent is the difference in the binding motif. The stress-related family members mentioned above bind to motifs containing the GCC box, which is commonly involved in stress-mediated responses, whereas AtRAP2.2 recognizes the motif ATCTA. Interestingly, the binding specificity for several AP2 domain-containing transcription factors appears to be very complex in vivo. This was concluded from a systematic approach conducted for the tomato transcription factor Pti4 for which binding of the GCC box was shown in vitro (Chakravarthy et al., 2003). Analysis of transcripts regulated by the overexpression of *Pti4* in Arabidopsis revealed that most of the promoters of Pti4-regulated genes did not contain a GCC box, leading to the hypothesis that *Pti4* might be able to recognize both GCC as well as non-GCC box-containing motifs. Data from other AP2/EREBP-overexpressing plants also indicate possible regulation of non-GCC box-containing genes (Wu et al., 2002; Tournier et al., 2003).

Regulatory factors, such as AtRAP2.2, may have the potential to improve complex multigene traits through genetically modified organism approaches or marker-assisted breeding for variation at the AtRAP2.2 locus. For AtRAP2.2, this might allow one to favorably alter the nutritional composition of crop plants by influencing entire biosynthetic pathways or improving agronomic properties. This is the case when those genes are master regulators of traits, such as the maize (*Zea mays*) LC/C1 transcription factors capable of increasing flavonol content in tomato (Bovy et al., 2002) or the Sub1A transcription factor conferring submergence tolerance in rice (*Oryza sativa*; Xu et al., 2006). The fact that AtRAP2.2 bound to at least *PSY* and *PDS* upstream regulatory sequences raised expectations for

its potential biotechnological value to modify provitamin A biosynthesis. However, our data indicate that AtRAP2.2 and SINAT2 are just two constituents of a significantly more complex regulatory network involved in carotenogenesis.

MATERIALS AND METHODS

South-Western Screening

A λZAPII cDNA-library of Arabidopsis (*Arabidopsis thaliana*; Kieber et al., 1993) was screened via South-western screening. As a radiolabeled probe, the primers 5′-caatctaaatatctaaaatataaa-3′ and 5′-tttatattttagatatttagattg-3′ were used to produce concatenated oligonucleotides according to Sambrook et al. (1989), resulting in concatemers of the sequence 5′-caatctaaatatctaaaatataaa-3′. Nitrocellulose filters were prepared in two sets; one set was used for the incubation with the radiolabeled probe directly, whereas the second copy was subjected to denaturation using 6 M GuHCl followed by renaturation (Vinson et al., 1988; Sambrook et al., 1989). Approximately 3×10^4 pfu per filter set were screened. Both filter sets were incubated for 12 h at 4°C with hybridization buffer, consisting of binding buffer (25 mM HEPES/KOH, pH 7.9; 7.5 mM $MgCl_2$; 20 mM KCl; 0.07 mM EDTA) containing 1 mM dithiothreitol (DTT), 0.25% (w/v) fat-free milk powder, and 10 μg mL^{-1} calf thyme DNA. The filters were washed 3 times for 5 min with 60 mL hybridization buffer before autoradiography. Clones showing a positive signal were isolated and used for subsequent rounds of screening.

Binding Assay with Recombinant AtRAP2.2

For gel retardation assays with recombinant AtRAP2.2, cDNA was subcloned into the expression vector pQE30 (Qiagen), yielding pQE30-AtRAP2.2, thereby providing the recombinant protein with an N-terminal 6×-His-tag. *Escherichia coli* (strain BL21) was transformed with pQE30-AtRAP2.2 and induced using isopropylthio-β-galactoside. Bacteria were lysed by two passages through a French press, centrifuged (13,000*g*/15 min), and the pellet was resuspended in 6 M GuHCl in binding buffer (see above). After 1-h incubation at room temperature, the mixture was recentrifuged and the supernatant was dialyzed against 50 volumes of binding buffer at 4°C overnight to allow protein renaturation. Gel retardation assays using 7 μg of protein were performed as described earlier (Welsch et al., 2003).

DNA Affinity Chromatography

Preparation of the AtRAP2.2 affinity chromatography column and binding of nuclear proteins was performed essentially as described (Kadonaga and Tjian, 1986; Koksharova and Wolk, 2002). The primers used for South-western screening described above were oligomerized by self ligation with T4 DNA ligase and coupled to cyanogen bromide-activated Sepharose 4B (Sigma). One milligram of nuclear proteins from Arabidopsis wild-type rosette leaves, isolated as described (Welsch et al., 2003), were diluted with an equal volume of buffer Z (25 mM HEPES/KOH, pH 7.8, 12.5 mM $MgCl_2$, 1 mM DTT, 20% [v/v] glycerol) and incubated with 440 μg poly[d(I-C)] for 1 h at 4°C. One milliliter of RAP DNA affinity resin was added, incubated overnight, washed four times with 2 mL of buffer Z containing 100 mM KCl, and bound proteins eluted using two 1.2-mL aliquots of buffer Z containing 1 M KCl. Eluates were combined, proteins were concentrated with TCA, and dissolved in 1% (v/v) SDS, 65 mM Tris/HCl, pH 7.0. Silver staining was performed using the ProteoSilver Plus silver stain kit (Sigma).

Plant Transformations and Growth of Plant Material

For pCAMBIA1390-nosP-AtRAP2.2, the *HPT* cDNA from pCAMBIA1390 was displaced with the *NPTII* cDNA from pCAMBIA2300, followed by a subcloning of the *AtRAP2.2* cDNA from the cDNA-containing pBluescript vector obtained by in vivo excision. For pCAMBIA1390-q35S-AtRAP2.2, four copies of the *CaMV-35S* enhancer regions in tandem were subcloned from the vector pTaq7 into the vector pCAMBIA1390, followed by subcloning of the *AtRAP2.2* cDNA. These vectors were used to transform Arabidopsis (ecotype Wassilewskija) plants by vacuum infiltration (Bechtold et al., 1993) using *Agrobacterium tumefaciens* strain GV3101 (Koncz and Schell, 1986). Homozygous T2 progeny were identified by the segregation pattern of the corresponding T3 progeny on hygromycin (30 μg mL^{-1}) or kanamycin (50 μg mL^{-1}) containing Murashige and Skoog plates. Heterozygous progeny of *rapΔutr* were verified by PCR on genomic DNA isolated from individual *rapΔutr* F3 progenies, using one *AtRAP2.2* gene-specific primer and one T-DNA-specific primer.

Transgenic lines and wild-type plants were grown simultaneously in aratrays (Lehle Seeds) under short-day conditions (8-h light/16-h dark, 22°C, 90 μmol m^{-2} s^{-1}) and watered by immersion three times per week. According to the classification system of Boyes et al. (2001), rosette leaves were harvested from 13 plants when they reached growth stage 5.10 (first flower buds visible). The leaves were pooled, frozen in liquid nitrogen, stored at −80°C, and used for further analysis. Root calli from wild-type and transgenic lines were generated in parallel according to Banno et al. (2001). For all samples, roots were cut from seedlings growing in at least two flasks of liquid medium and transferred onto three plates containing callus induction medium. After 4 weeks, calli from all three plates were pooled, ground in liquid nitrogen, and stored at −80°C. All samples were produced twice for use as biological replicates.

Carotenoid Extraction and Quantification

The lipophilic compounds of 5 mg lyophilized leaf or 100 mg root callus material, respectively, were extracted three times by adding 2 mL of acetone and sonicating. One hundred microliters of α-tocopherolacetate (2 mg mL^{-1} in acetone; Sigma) were added as an internal standard. After centrifugation (5 min/6,000*g*), the acetone phases were pooled and dried by rotary evaporation; pigments were resuspended in 2 mL petroleum ether:diethyl ether (2:1 [v/v]); 1 mL of water was added and the samples were centrifuged (5 min/6,000*g*). The organic phase was dried and the pigments were dissolved in 30 μL chloroform. Ten microliters of each sample were subjected to quantitative analysis using HPLC with a C30 reversed-phase column (YMC Europe GmbH) and a gradient system as described (Hoa et al., 2003). Carotenoids were identified by their absorption spectra using a photodiode array detector (PDA 2996; Waters). Normalization of the samples to the internal standard and quantification of carotenoid amounts were performed as described previously (Schaub et al., 2005).

RNA Extraction, Microarray Experiments, and Data Analysis

Total RNA was isolated using Concert reagent (Invitrogen). RNA cleanup and on-column DNAseI digestion was performed using the Qiagen RNeasy mini kit. After RNA quality control by formaldehyde agarose gel analysis, biotinylated target RNA (cRNA) was prepared from 15 μg of total RNA using the Affymetrix GeneChip one-cycle target labeling kit (Affymetrix). Two biological replicates for each line were hybridized to the Affymetrix Arabidopsis ATH1 GeneChip. GeneChip Suite 5.0 (Affymetrix) was used for data normalization using default settings. The target intensity for all probe sets of each array was scaled to 500. GeneChip data files were imported into GeneSpring 7.2 (Agilent Technologies) for further analyses.

Two normalization steps were applied to each sample. First, per-chip normalization was performed using the fiftieth percentile of all measurements to adjust total signal intensity in each chip. Second, per-gene normalization using the median for each gene was applied. For analysis, data filtration based on flags present in at least three of four samples used for comparison (wild-type and overexpressing line, two biological replicates each) was first performed and a corresponding gene list based on those flags was generated. Statistically significant changes in mRNA abundance were determined using the statistical package with GeneSpring 7.2. Statistical significance was determined by ANOVA analysis using a P value of 0.05 as the cutoff. Lists of genes that were either induced or suppressed more than 2.5-fold between wild-type versus transgenic lines were created by filtration-on-fold function within the presented list. For a less stringent analysis (see Supplemental Table S1), data filtration was based on flags present and marginal in at least one of four samples used for comparison; statistical analysis and filtration on 2.5-fold difference was performed as described. The intersection of both gene lists was obtained using the Venn diagram function of GeneSpring 7.2.

Affymetrix GeneChip data were deposited at the ArrayExpress (http://www.ebi.ac.uk/arrayexpress) database in compliance with Minimum Informa-

tion About a Microarray Experiment standards with accession number E-TABM-209.

TaqMan Real-Time RT-PCR Assay

Total RNA was extracted as described above. First-strand cDNA synthesis was performed using the TaqMan RT reagents (Applied Biosystems) according to the manufacturer's protocol. Primers and TaqMan MGB probes were designed from cDNA sequences of Arabidopsis, using Primer Express software (Applied Biosystems). The following primers and probes were used: AtRAP2.2 forward, 5′-gatgatgatgtcttcgtcaatgttaa-3′; reverse, 5′-gcggaagctacgggcttagt-3′; probe, 5′-tttcgtcttcaccgcaac-3′; PSY forward, 5′-gtggtcgtcctttcgatatgc-3′; reverse, 5′-cgaccgggtatctagcaactg-3′; probe, 5′-tgatgctgctctcgc-3′; PDS forward, 5′-gttgcacttccccacctagtg-3′; reverse, 5′-cctccggaaaggctttgtatg-3′; probe, 5′-tcgaatatgatccactactg-3′.

Specific mRNA levels were quantified by real-time RT-PCR (ABI Prism 7000; Applied Biosystems) using 18S rRNA levels for normalization. For 18S rRNA quantification, the eukaryotic 18S rRNA endogenous control kit (Applied Biosystems) was used. Reporter (5′ end) dyes for the TaqMan MGB probes were 6FAM, except for 18S rRNA, where VIC was used. The relative quantity of the transcripts was calculated by using the comparative threshold cycle method (Livak, 1997). Data were normalized first to the corresponding 18S rRNA levels and then expressed as relative to the wild-type transcript levels.

Protein Overlay Assay

pGEM4 constructs were used for coupled transcription and translation using the TNT SP6 coupled RL and WG extract system (Promega) in the presence of [^{35}S]Met and [^{35}S]Cys (GE Healthcare) according to the supplier's protocol to generate [^{35}S]-labeled proteins.

Nuclear extracts from illuminated mustard (*Sinapis alba*) seedlings were isolated as described (Welsch et al., 2003). Protein concentration was determined using Bio-Rad protein assay. Thirty micrograms of nuclear proteins were separated on SDS-PAGE and transferred onto nitrocellulose membrane. Membranes were blocked with prehybridization buffer (3% [w/v] bovine serum albumin, 50 mM Tris-HCl, pH 7.5, 150 mM NaCl, 0.005% [v/v] Tween 20) overnight at 4°C. The solution was then replaced with 5×10^5 cpm [^{35}S]-labeled in vitro-translated AtRAP2.2 in prehybridization buffer and incubated overnight at 4°C. Membranes were rinsed three times for 5 min at room temperature in prehybridization buffer, air dried, and exposed to a PhosphorImager screen (Fuji Film) to visualize radiolabeled proteins.

Yeast Two-Hybrid Assay

Constructs to test for autoactivation were produced by subcloning the AtRAP2.2 cDNA into the vector pGBT9, truncation were constructed by using appropriate restriction sites or by amplification and subcloning PCR fragments using mutagenized primers. Yeast (*Saccharomyces cerevisiae*) two-hybrid screening was performed using the MATCHMAKER GAL4 two-hybrid system (CLONTECH). An Arabidopsis (ecotype Columbia-0) MATCHMAKER cDNA library present in the vector pGAD424 and the bait vector pGBT9-RAP1-166 were sequentially transformed into the yeast reporter strain Hf7c and cultured on synthetic dropout agar lacking Leu, Trp, and His. Yeast transformants that appeared on selection medium within 2 d were transferred on fresh selection plates and allowed to grow for two more days. From these potential transformants, 61 yeast clones that grew on selection medium were tested for β-galactosidase activity by the colony-lift filter assay with 5-bromo-4-chloro-3-indolyl-β-D-galactopyranoside. Plasmids were rescued from 20 *His-/lacZ* yeast transformants and identical cDNAs were identified by restriction analysis. Interaction was retested by cotransformation of the selected pGAD424-cDNA plasmids with pGBT9-RAP1-166 into Hf7c followed by both His and lacZ assays. As a final test, selected pGAD424-cDNA plasmids were cotransformed with the empty pGBT9 vector into the Hf7c yeast strain to check for possible autoactivation of the gene product.

Pull-Down Assays

Recombinant GST, GST-SINAT2-C, and GST-SINAT2, bound onto glutathione-Sepharose beads (GE Healthcare) were produced according to Frangioni and Neel (1993) using 0.5% (w/v) *N*-laurylsarcosyl and 1% (v/v) Triton X-100. To equal amounts of GST or GST fusion protein, respectively, 5 μL of in vitro-translated [^{35}S]-labeled AtRAP2.2 were added. Fifty microliters of 5× hybridization buffer (100 mM Tris/HCl, pH 8.0; 500 mM NaCl, 5 mM DTT, 5 mM EDTA) and 200 μL water were added and incubated with light agitation for 20 min at room temperature. After centrifugation at 500*g*/4°C for 2 min, the pellet was washed five times with wash buffer (150 mM NaCl, 10 mM Tris/HCl, pH 8.0; 1 mM EDTA, 1 mM phenylmethylsulfonyl fluoride; 1 mM DTT; 1 μg μL^{-1} leupeptin, 1 μg μL^{-1} antipain, 10% [v/v] glycerol). The pellet was resuspended in 25 μL SDS sample buffer, boiled for 5 min, subjected to SDS-PAGE, and transferred onto nitrocellulose membranes. A PhosphorImager screen was used to visualize radiolabeled proteins.

Protein Extraction and Western-Blot Analysis

For protein extraction, 100 mg of plant material were ground in liquid nitrogen and resuspended in 150 μL 40% (w/v) Suc. Four hundred microliters of phenol, 10 μL 10% (w/v) SDS, and 20 μL β-mercaptoethanol were added, the sample was vortexed, incubated for 10 min at 58°C, and centrifuged for 3 min at 800*g*. Proteins were precipitated by adding 10 volumes of methanol and centrifugation for 5 min at 3,300*g*, washed, dried, and resuspended in sample buffer (65 mM Tris/HCl, pH 7.0, 1% [w/v] SDS). Protein concentration was determined with Bio-Rad protein assay; equal amounts were separated by SDS-PAGE and blotted onto nitrocellulose membrane. The membrane was blocked overnight in Tris-buffered saline containing 5% (w/v) milk powder. Analysis of actin protein amounts was carried out using monoclonal antiactin antibodies (Sigma) and using the enhanced chemiluminescence detection system (GE Healthcare) according to the manufacturer's instructions. The western blot was stripped and reprobed with anti-AtRAP2.2 antibodies; analysis was carried out using the alkaline phosphatase system.

For generation of anti-AtRAP2.2 antibodies, the N-terminal 166 amino acids of AtRAP2.2 were expressed as a GST fusion protein in the vector pGEX4T in *E. coli* BL21 and purified using glutathione-Sepharose beads according to Frangioni and Neel (1993). GST fusion protein was separated from copurified GST by SDS-PAGE followed by electroelution and used for the immunization of five mice.

Sequence data from this article can be found in the GenBank/EMBL data libraries under accession numbers At3g14230 (*AtRAP2.2*) and At3g58040 (*SINAT2*).

Supplemental Data

The following materials are available in the online version of this article.

Supplemental Figure S1. SIAH proteins from Arabidopsis.

Supplemental Table S1. SINA-homologous proteins from Arabidopsis.

ACKNOWLEDGMENTS

We thank Syngenta, Inc., for making the SAIL collection available, the Arabidopsis Biological Resource Center for the λZAPII cDNA library, and Thomas Merkle (University of Bielefeld) for supplying the Arabidopsis cDNA library for two-hybrid screening. We gratefully acknowledge Maria Magallanes-Lundback (Michigan State University) for making the cRNA preparation and Affymetrix GeneChip hybridization.

Received June 28, 2007; accepted September 10, 2007; published September 14, 2007.

LITERATURE CITED

Al-Babili S, Hoa TT, Schaub P (2006) Exploring the potential of the bacterial carotene desaturase CrtI to increase the β-carotene content in Golden Rice. J Exp Bot **57:** 1007–1014

Aukerman MJ, Sakai H (2003) Regulation of flowering time and floral organ identity by a microRNA and its APETAL2-like target genes. Plant Cell **15:** 2730–2741

Banno H, Ikeda Y, Niu QW, Chua NH (2001) Overexpression of Arabidopsis ESR1 induces initiation of shoot regeneration. Plant Cell **13:** 2609–2618

Bechtold N, Ellis J, Pelletier G (1993) *In planta* Agrobacterium mediated gene transfer by infiltration of adult *Arabidopsis thaliana* plants. CR Acad Sci Paris Life Sciences **316:** 1194–1199

Boulton SJ, Brook A, Staehling-Hampton K, Heitzler P, Dyson N (2000) A role for Ebi in neuronal cell cycle control. EMBO J **19:** 5376–5386

Bovy A, de Vos R, Kemper M, Schijlen E, Pertejo MA, Muir S, Collins G, Robinson S, Verhoeyen M, Hughes S, et al (2002) High-flavonol tomatoes resulting from the heterologous expression of the maize transcription factor genes LC and C1. Plant Cell **14:** 2509–2526

Boyes DC, Zayed AM, Ascenzi R, McCaskill AJ, Hoffman NE, Davis KR, Gorlach J (2001) Growth stage-based phenotypic analysis of Arabidopsis: a model for high throughput functional genomics in plants. Plant Cell **13:** 1499–1510

Carthew RW, Rubin GM (1990) Seven in absentia, a gene required for specification of R7 cell fate in the Drosophila eye. Cell **63:** 561–577

Chakravarthy S, Tuori R, D'Ascenzo MD, Fobert PR, Després C, Martin GB (2003) The tomato transcription factor Pti4 regulates defense-related gene expression via GCC box and non-GCC box *cis* elements. Plant Cell **15:** 3033–3050

Chen X (2004) A microRNA as a translational repressor of APETALA2 in Arabidopsis flower development. Science **303:** 2022–2025

Dong X, Tsuda L, Zavitz KH, Lin M, Li S, Carthew RW, Zipursky SL (1999) ebi regulates epidermal growth factor receptor signaling pathways in Drosophila. Genes Dev **13:** 954–965

Frangioni JV, Neel BG (1993) Solubilization and purification of enzymatically active glutathione *S*-transferase (pGEX) fusion proteins. Anal Biochem **210:** 179–187

Hoa TT, Al-Babili S, Schaub P, Potrykus I, Beyer P (2003) Golden Indica and Japonica rice lines amenable to deregulation. Plant Physiol **133:** 161–169

Howitt CA, Pogson BJ (2006) Carotenoid accumulation and function in seeds and non-green tissues. Plant Cell Environ **29:** 435–445

Jung J, Won SY, Suh SC, Kim H, Wing R, Jeong Y, Hwang I, Kim M (2007) The barley ERF-type transcription factor HvRAF confers enhanced pathogen resistance and salt tolerance in *Arabidopsis.* Planta **225:** 575–588

Kadonaga JT, Tjian R (1986) Affinity purification of sequence-specific DNA binding proteins. Proc Natl Acad Sci USA **83:** 5889–5893

Kieber JJ, Rothenberg M, Roman G, Feldmann KA, Ecker JR (1993) CTR1, a negative regulator of the ethylene response pathway in Arabidopsis, encodes a member of the raf family of protein kinases. Cell **72:** 427–441

Koksharova OA, Wolk CP (2002) Novel DNA-binding proteins in the cyanobacterium Anabaena sp. strain PCC 7120. J Bacteriol **184:** 3931–3940

Koncz C, Schell J (1986) The promoter of T_L-DNA gene 5 controls the tissue-specific expression of chimeric genes carried by a novel type of Agrobacterium binary vector. Mol Gen Genet **204:** 383–396

Kosarev P, Mayer KFX, Hardtke CS (2002) Evaluation and classification of RING-finger domains encoded by the Arabidopsis genome. Genome Biol **3:** RESEARCH0016

Laity JH, Lee BM, Wright PE (2001) Zinc finger proteins: new insights into structural and functional diversity. Curr Opin Struct Biol **11:** 39–46

Lee JH, Kim DM, Lee JH, Kim J, Bang JW, Kim WT, Pai HS (2005) Functional characterization of NtCEF1, an AP2/EREBP-type transcriptional activator highly expressed in tobacco callus. Planta **222:** 211–224

Li S, Li Y, Carthew RW, Lai ZC (1997) Photoreceptor cell differentiation requires regulated proteolysis of the transcriptional repressor tramtrack. Cell **90:** 469–478

Livak KJ (1997) User Bulletin No. 2: ABI PRISM 7700 Sequence Detection System. PE Applied Biosystems, Foster City, CA, pp 11–15

Paine JA, Shipton CA, Chaggar S, Howells RM, Kennedy MJ, Vernon G, Wright SY, Hinchliffe E, Adams JL, Silverstone AL, et al (2005) Improving the nutritional value of Golden Rice through increased pro-vitamin A content. Nat Biotechnol **23:** 482–487

Reed JC, Ely KR (2002) Degrading liaisons: SIAH structure revealed. Nat Struct Biol **9:** 8–10

Riechmann JL, Meyerowitz EM (1998) The AP2/EREBP family of plant transcription factors. Biol Chem **379:** 633–646

Sambrook J, Fritsch EF, Maniatis T (1989) Molecular Cloning: A Laboratory Manual, Ed 2. Cold Spring Harbor Laboratory, Cold Spring Harbor, NY

Schaub P, Al-Babili S, Drake R, Beyer P (2005) Why is golden rice golden (yellow) instead of red? Plant Physiol **138:** 441–450

Szabó I, Bergantino E, Giacometti GM (2005) Light and oxygenic photosynthesis: energy dissipation as a protection mechanism against photooxidation. EMBO Rep **6:** 629–634

Tang AH, Neufeld TP, Kwan E, Rubin GM (1997) PHYL acts to downregulate TTK88, a transcriptional repressor of neuronal cell fates, by a SINA-dependent mechanism. Cell **90:** 459–467

Tournier B, Sanchez-Ballesta MT, Jones B, Pesquet E, Regad F, Latché A, Pech JC, Bouzayen M (2003) New members of the tomato ERF family show specific expression pattern and diverse DNA-binding capacity to the GCC box element. FEBS Lett **28:** 149–154

Vinson CR, LaMarco KL, Johnson PF, Landschulz WH, McKnight SL (1988) In situ detection of sequence-specific DNA binding activity specified by a recombinant bacteriophage. Genes Dev **2:** 801–806

von Lintig J, Welsch R, Bonk M, Giuliano G, Batschauer A, Kleinig H (1997) Light-dependent regulation of carotenoid biosynthesis occurs at the level of phytoene synthase expression and is mediated by phytochrome in Sinapis alba and Arabidopsis thaliana seedlings. Plant J **12:** 625–634

Wang XJ, Reyes JL, Chua NH, Gaasterland T (2004) Prediction and identification of Arabidopsis thaliana microRNAs and their mRNA targets. Genome Biol **5:** R65

Weigel D (1995) The APETALA2 domain is related to a novel type of DNA binding domain. Plant Cell **7:** 388–389

Welsch R, Beyer P, Hugueney P, Kleinig H, von Lintig J (2000) Regulation and activation of phytoene synthase, a key enzyme in carotenoid biosynthesis, during photomorphogenesis. Planta **211:** 846–854

Welsch R, Medina J, Giuliano G, Beyer P, von Lintig J (2003) Structural and functional characterization of the phytoene synthase promoter from Arabidopsis. Planta **216:** 523–534

Wu K, Tian L, Hollingworth J, Brown DC, Miki B (2002) Functional analysis of tomato Pti4 in Arabidopsis. Plant Physiol **128:** 30–37

Xie Q, Guo HS, Dallman G, Fang S, Weissman AM, Chua NH (2002) SINAT5 promotes ubiquitin-related degradation of NAC1 to attenuate auxin signals. Nature **419:** 167–170

Xu K, Xu X, Fukao T, Canlas P, Maghirang-Rodriguez R, Heuer S, Ismail AM, Bailey-Serres J, Ronald PC, Mackill DL (2006) Sub1A is an ethylene-response-factor-like gene that confers submergence tolerance to rice. Nature **442:** 705–708

Zhang H, Huang Z, Xie B, Chen Q, Tian X, Zhang X, Zhang H, Lu X, Huang D, Huang R (2004) The ethylene-, jasmonate-, abscisic acid- and NaCl-responsive tomato transcription factor JERF1 modulates expression of GCC box-containing genes and salt tolerance in tobacco. Planta **220:** 262–270

Zheng N, Schulman BA, Song L, Miller JJ, Jeffrey PD, Wang P, Chu C, Koepp DM, Elledge SJ, Pagano M, et al (2002) Structure of the Cul1–Rbx1–Skp1–F box^{Skp2} SCF ubiquitin ligase complex. Nature **416:** 703–709